A solution-processable bipolar molecular glass as a host material for white electrophosphorescent devices

Chen-Han Chien,[a] Liang-Rern Kung,[a] Chen-Hao Wu,[a] Ching-Fong Shu,*[a] Sheng-Yuan Chang[b] and Yun Chi*[b]

Received 11th March 2008, Accepted 16th May 2008
First published as an Advance Article on the web 16th June 2008
DOI: 10.1039/b804192j

A solution-processable bipolar material **tBu-OXDTFA** comprising an electron-rich triphenylamine core and electron-deficient oxadiazole/fluorene peripheries was synthesized. This dendrimer-like molecule not only possesses a high triplet energy (2.74 eV) but also exhibits excellent film-forming properties upon solution processing. We achieved highly efficient white electrophosphorescent OLEDs (22.3 cd A^{-1}, 11.6%) through solution processing, wherein the single white emitting layer was readily formed after spin-coating a solution of blue- and red-phosphor co-dopants containing **tBu-OXDTFA** as the host matrix.

Introduction

Organic light-emitting diodes (OLEDs) have attracted considerable interest because of their potential applications in flat-panel displays and in solid state lighting.[1] Phosphorescent emitters are considered to be superior to their fluorescent counterparts at improving the efficiency of electroluminescent (EL) devices; because they can harvest both singlet and triplet excitons, their internal quantum efficiencies can reach theoretical levels as high as 100%.[2] In phosphorescent OLEDs, the triplet emitters are normally used as emitting guests in a host material to reduce the self-quenching associated with the relatively long excited state lifetimes of triplet emitters and triplet–triplet annihilation;[3] consequently, the choice of host materials is of vital importance for the preparation of efficient phosphorescent OLEDs.

Presently, most electroluminescent devices are fabricated using vacuum deposition, which is a complicated and expensive manufacturing process. In contrast, solution processing methods, such as spin-coating and ink-jet printing, are relatively inexpensive and can be utilized for the preparation of large-area displays.[4] Most studies have employed solution-processable polymeric host materials, such as poly(9-vinylcarbazole) and polyfluorenes, blended with phosphorescent emitters as the emitting layer (EML).[5] Nevertheless, several issues—such as aggregation or phase separation of the phosphor in the macromolecular matrix and the intrinsic difficulty in purifying the polymeric materials—can hamper the applicability of polymeric hosts.[6]

In this paper, we report the design and synthesis of a solution-processable, bipolar molecular glass, namely **tBu-OXDTFA**, for use as a host material in electrophosphorescent devices. As shown in Scheme 1, **tBu-OXDTFA** comprises a triphenylamine (TPA) core and fluorene/oxadiazole (OXD) peripheries. These individual building blocks each exhibit a high triplet energy

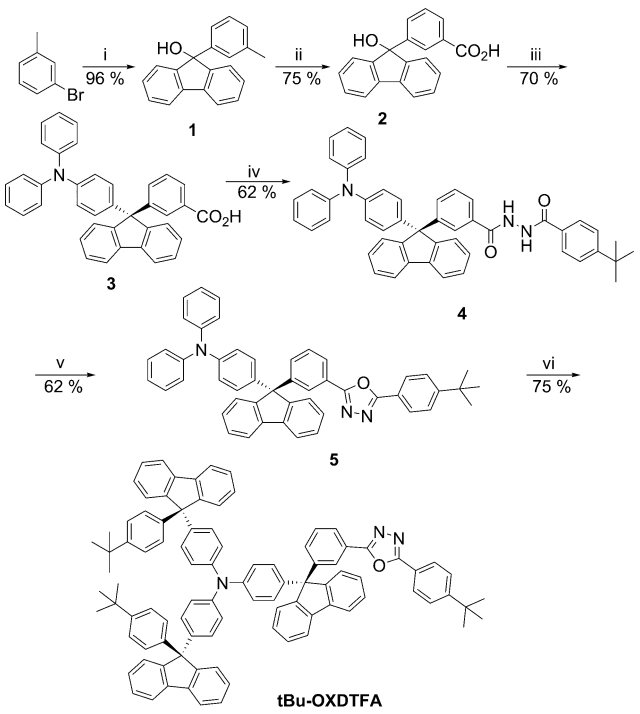

Reagents: (i) a) Mg, Et_2O b) 9-fluorenone (ii) $KMnO_4$, pyridine, H_2O (iii) TPA, CH_3SO_3H, 1,4-dioxane (iv) a) *i*-BuOCOCl, NMM, THF b) *t*-BuPhCONHNH$_2$ (v) Ph_3P, CBr_4, CH_2Cl_2 (vi) **6**, CH_3SO_3H, CH_2Cl_2.

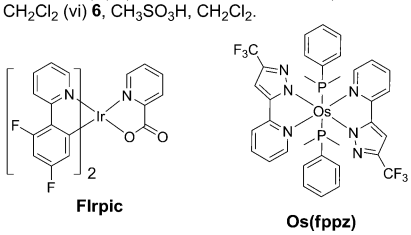

Scheme 1 Synthesis route to **tBu-OXDTFA** and chemical structures of FIrpic and Os(fppz).

(E_T > 2.9 eV)[7] and are connected through the sp^3-hybridized C-9 atoms to effectively interrupt any extended π-conjugation. This structural feature endows **tBu-OXDTFA** with an adequately high

[a]*Department of Applied Chemistry, National Chiao Tung University, Hsin-Chu, Taiwan 30050*
[b]*Department of Chemistry, National Tsing Hua University, 300 Hsinchu, Taiwan*

value of E_T for efficient confinement of the triplet excitons primarily on the guest, blue-emitting phosphors. In addition, the built-in bipolar functionalities, arising from the electron-rich TPA core and electron-deficient OXD pendent units, may facilitate and balance the hole and electron injection and transport, respectively.[8] Moreover, the three-dimensional, rigid, and asymmetric structure of **tBu-OXDTFA** hinders its close packing and suppresses its crystallizability, leading to an amorphous material exhibiting pronounced thermal stability. We prepared highly efficient white electrophosphorescent OLEDs (22.3 cd A^{-1}, 11.6%) through solution processing; the single white EML was formed simply through spin-coating of a solution of blue- and red-phosphor co-dopants containing **tBu-OXDTFA** as the host matrix.

Results and discussion

Synthesis

Scheme 1 illustrates the synthesis route followed for the preparation of **tBu-OXDTFA**. The Grignard reaction of fluorenone with *m*-tolylmagnesium bromide gave the corresponding alcohol, 9-(*m*-tolyl)fluoren-9-ol (**1**), the tolyl group of which was then oxidized using $KMnO_4$ in H_2O/pyridine to provide the carboxylic acid **2**. Subsequent Friedel–Crafts-type substitution of triphenylamine with **2** yielded compound **3**. This reaction proceeded through the initial formation of a transitory carbocation from the protonated 9-fluorenol group,[9] which in turn underwent electrophilic substitution exclusively at the electron-rich para carbon atom of the TPA phenyl group. The formation of the OXD moiety commenced from the acid **3** in a two-step protocol: the acylhydrazide and **3** were coupled under amide bond-forming conditions, followed by cyclodehydration mediated by CBr_4 and Ph_3P.[10] Finally, the oxadiazole **5** was subjected to another Friedel–Crafts reaction with 9-(4-*tert*-butylphenyl)-9-fluorenol (**6**)[11] to afford the desired host material **tBu-OXDTFA**. The structure of **tBu-OXDTFA** was characterized using ^1H and ^{13}C NMR spectroscopy, elemental analysis, and high-resolution mass spectrometry.

Thermal properties

We used thermogravimetric analysis (TGA) and differential scanning calorimetry (DSC) to investigate the thermal properties of **tBu-OXDTFA** (Fig. 1). TGA indicated that its 5 and 10% weight losses occurred at 408 and 426 °C, respectively. DSC revealed that **tBu-OXDTFA** exhibited an extremely high glass transition temperature of 207 °C with no detectable values of T_c and T_m at temperatures up to 370 °C. This observation indicates the prominent stability of the amorphous glass state of **tBu-OXDTFA**, which we attribute to the presence of its rigid fluorene and OXD peripheries and its high molecular weight. In addition, the presence of the propeller-like TPA core hinders close packing of **tBu-OXDTFA**, suppressing its crystallizability.[12] To investigate its morphology, we prepared thin films of **tBu-OXDTFA** through spin-coating from a chlorobenzene solution onto silicon wafers and imaged them using atomic force microscopy (AFM; Fig. 2). The surface topographies clearly revealed that the spin-coated films exhibited fairly smooth and pinhole-free surface morphologies, with a root-mean-square (RMS) surface roughness of 0.306 nm. For a spin-coated, white-emitting **tBu-OXDTFA** film doubly doped with 14 wt% FIrpic and 0.1 wt% Os(fppz),[13] we calculated the RMS surface roughness to be 0.359 nm; there was no phase separation or any aggregated domains. These results demonstrate that **tBu-OXDTFA** is capable of forming amorphous films through solution processing, with organometallic triplet emitters dispersed homogeneously.

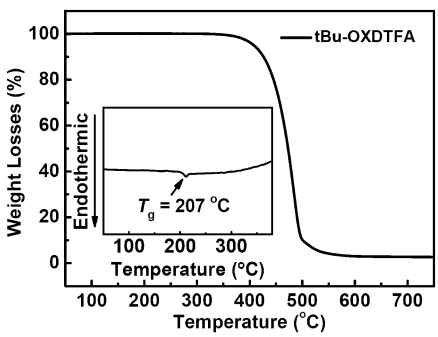

Fig. 1 TGA trace of **tBu-OXDTFA** recorded at a heating rate of 10 °C min^{-1}. Inset: DSC measurement recorded at a heating rate of 10 °C min^{-1}.

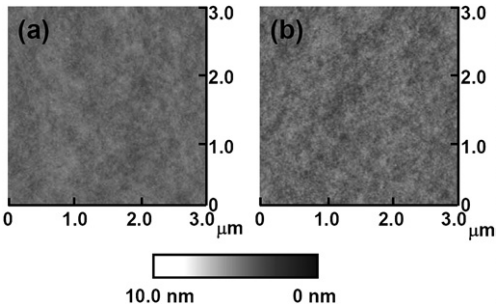

Fig. 2 AFM topographic images (tapping mode) of (a) neat **tBu-OXDTFA** and (b) **tBu-OXDTFA** doped with 14 wt% FIrpic and 0.1 wt% Os(fppz). The films were prepared through spin-coating from chlorobenzene solutions onto silicon wafers.

Electrochemistry

We employed cyclic voltammetry (CV) to investigate the electrochemical behavior of **tBu-OXDTFA**, using ferrocene as the internal standard. During the anodic scan in CH_2Cl_2, a reversible oxidative process occurred at 0.42 V ($E^{o\prime}$), originating from the oxidation of the electron-rich TPA core. Upon the cathodic sweep in THF, we detected a reversible reductive process at −2.60 V ($E^{o\prime}$), attributable to reduction of the peripheral electron-deficient OXD units (Fig. 3). This reversible reductive and oxidative behavior indicates that **tBu-OXDTFA** can be utilized as both a hole and an electron transporter. Moreover, such pronounced electrochemical stability, which improves the lifetime of electroluminescent devices, makes **tBu-OXDTFA** a desirable host material for use in light-emitting applications.

Photophysical properties

Fig. 4a displays the absorption and PL spectra of **tBu-OXDTFA** in various organic solvents. In CH_2Cl_2, the absorption spectrum

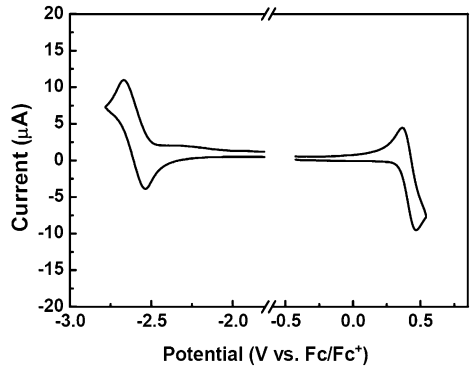

Fig. 3 Cyclic voltammogram of **tBu-OXDTFA** recorded at a scanning rate of 50 mV s^{-1}.

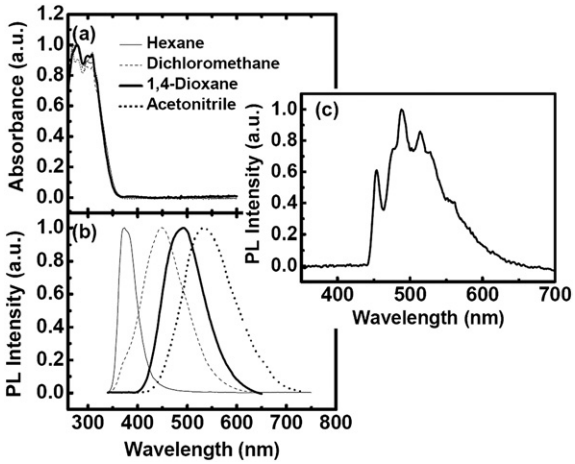

Fig. 4 (a) UV-Vis absorption and (b) PL spectra of **tBu-OXDTFA** in various organic solvents. (c) Normalized phosphorescence spectrum (77 K) of **tBu-OXDTFA** in 2-MeTHF.

of **tBu-OXDTFA** is almost a superimposed image of the absorptions of the fluorene-substituted TPA group and the OXD unit, suggesting that negligible interactions occur between the TPA and OXD moieties in the ground state. Furthermore, in all the solvents studied, the features in the absorption spectra were nearly identical and independent of the solvent polarity, indicating that the Franck–Condon excited state of **tBu-OXDTFA** was subject to a rather small dipolar change with respect to the ground state. In contrast, the PL spectra exhibit a strong dependence on the solvent polarity, with the emission band red-shifting significantly upon increasing the solvent polarity (Fig. 4b). We attribute this phenomenon to a mechanism involving a fast photoinduced electron transfer between the designed donor (TPA)–acceptor (OXD) pairs, leading to a large change in the dipole moment in the excited state; a subsequent solvent relaxation process results in the solvent polarity-dependent emission.[14] To evaluate the potential of utilizing **tBu-OXDTFA** as a host material in phosphorescent OLEDs, we measured its phosphorescence spectrum in a frozen 2-methyltetrahydrofuran (2-MeTHF) matrix at 77 K (Fig. 4c). We used the highest-energy 0–0 phosphorescent emission, located at 2.74 eV, to calculate the E_T gap of **tBu-OXDTFA**, giving a value higher than that reported for the common triplet blue-emitter FIrpic (2.65 eV).[15] Accordingly, this value of E_T is sufficiently high to effectively confine the triplet excitons on the guest and prevent back energy transfer to the host molecules; thus, we expected that **tBu-OXDTFA** would serve as an appropriate host for short-wavelength dopants, such as FIrpic, as well as long-wavelength dopants.[16]

Electroluminescence properties of OLEDs

To assess the utility of this solution-processable compound as a host material in OLEDs, we fabricated a white light-emitting device having the configuration ITO/PEDOT (35 nm)/EML (60–80 nm)/1,3,5-tris(*N*-phenylbenzimidazol-2-yl)benzene (TPBI, 30 nm)/LiF (15 Å)/Al (100 nm). The EML—a **tBu-OXDTFA** film doped with blue-emitting FIrpic (14 wt%) and red-emitting Os(fppz) (0.1 wt%)—was prepared readily through spin-coating from a chlorobenzene solution consisting of the co-dopants and the host material. The TPBI layer was employed as an electron-transporting and hole-blocking layer. As illustrated in Fig. 5, the EL spectrum exhibits dual emissions—with equalized blue and red emission intensities—covering the whole visible region. The Commission Interationale d'Eclairage (CIE) chromaticity coordinates of the EL emission at a bias of 11 V were (0.37, 0.39), *i.e.*, in the white light region and close to the equienergy white point. When we increased the driving voltage to 17 V, the CIE coordinates of the emission color remained almost constant and the EL spectrum barely changed. Fig. 6a presents the current density–voltage–luminance (*I–V–L*) curves of the **tBu-OXDTFA**-based device, which was turned on at 5.9 V (corresponding to 1 cd m^{-2}) and had a maximum brightness of 20 280 cd m^{-2}. As revealed in Fig. 6b, the maximum external quantum efficiency (max. η_{ext}) of this white-emitting device was 11.6% (953 cd m^{-2}, 4.27 mA cm^{-2}), and the corresponding luminance and power efficiencies were 22.3 cd A^{-1} and 5.0 lm W^{-1}. Even at brightnesses beyond 10 000 cd m^{-2}, 80% of the peak efficiency (9.2%) was sustained, along with a luminescence efficiency of 17.6 cd A^{-1}. We attribute this high performance to the presence of both electron-rich TPA and electron-deficient OXD units in **tBu-OXDTFA**, which may improve and balance charge injection and transport, leading to efficient charge recombination. Moreover, the short triplet excited lifetime of Os(fppz) (*ca.* 0.7 μs)[13] assists in this high performance because it prevents undesired T–T and P–T annihilation from occurring under high current densities.[3]

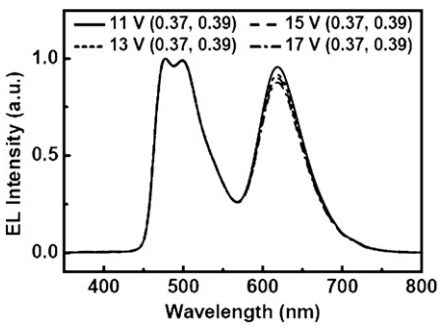

Fig. 5 EL spectra of a **tBu-OXDTFA**-based device co-doped with 14 wt% FIrpic and 0.1 wt% red-emitting Os(fppz), recorded at various driving voltages.

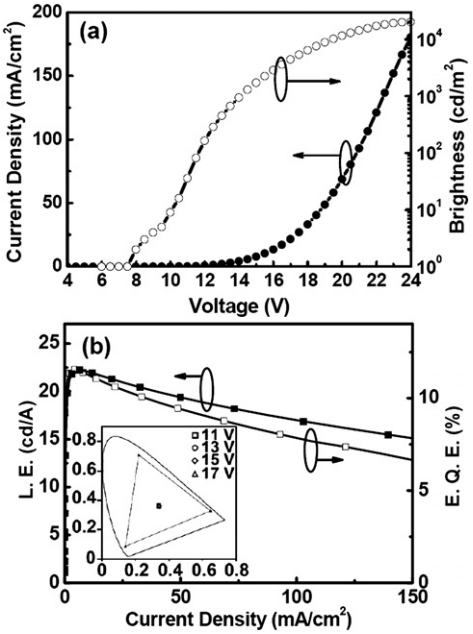

Fig. 6 (a) Current density–voltage–luminance and (b) luminance efficiency–current density–external quantum efficiency plots of the **tBu-OXDTFA**-based device.

Conclusions

In conclusion, we have synthesized and characterized a bipolar host material, **tBu-OXDTFA**, containing both hole- and electron-transporting functionalities. This dendrimer-like structure exhibits not only a high triplet energy but also good film-forming properties for solution processing. We achieved highly efficient white electrophosphorescent OLEDs (22.3 cd A^{-1}, 11.6%) through solution processing, wherein the single white EML was readily formed after spin-coating a solution containing **tBu-OXDTFA** and two co-dopants [blue-emitting FIrpic and red-emitting Os(fppz)]. In this paper we demonstrate that utilizing a dendritic small molecule, **tBu-OXDTFA**, as a host co-doped with organometallic phosphors allows the ready fabrication of white electrophosphorescent OLEDs possessing simple device structures, yet exhibiting high efficiency and luminance.

Experimental

General directions

All chemicals were purchased from Aldrich, TCI, and Acros Organics and used without further purification. Column chromatography was performed on silica gel (E. Merck Art. 7734 silica gel, 60 particle size, 70–230 mesh ASIM). NMR spectra were recorded on Varian UNITY INOVA 500 MHz, Varian Unity 300 MHz, and Bruker-DRX 300 MHz spectrometers. Chemical shifts are denoted on the scale in ppm, with reference to $CDCl_3$ or CD_3COCD_3. Mass spectra were obtained using JEOL JMS-HX 110 and SX-102A mass spectrometers. Differential scanning calorimetry (DSC) was performed using a Seiko EXSTAR 6000 DSC unit operated at heating and cooling rates of 10 and 50 °C min^{-1}, respectively. The glass transition temperatures (T_g) were determined from the second heating scan. Thermogravimetric analysis (TGA) was undertaken using a DuPont TGA 2950 instrument. The thermal stabilities of the samples under a nitrogen atmosphere were determined by measuring their weight losses while heating at a rate of 10 °C min^{-1}. UV-Vis spectra were measured using an HP 8453 diode-array spectrophotometer. PL spectra were obtained using a Hitachi F-4500 luminescence spectrometer. The low-temperature phosphorescence spectrum was obtained using a composite spectrometer containing a monochromator (Jobin Yvon, Triax 190) coupled to a liquid nitrogen-cooled charge-coupled device (CCD) detector (Jobin Yvon, CCD-1024 × 256-open-1LS). Cyclic voltammetry (CV) measurements were performed using a BAS 100 B/W electrochemical analyzer; 0.1 M tetrabutylammonium hexafluorophosphate ($TBAPF_6$) was the supporting electrolyte. The potentials were measured against an Ag/Ag^+ (0.01 M $AgNO_3$) reference electrode with ferrocene as the internal standard. Atomic force microscopy measurements were performed in the tapping mode under ambient conditions using a Digital Nanoscope IIIa instrument.

Device fabrication

PEDOT was spin-coated directly onto indium tin oxide (ITO) glass and dried at 80 °C for 12 h under vacuum to improve both the hole injection capability and the smoothness of the substrate. The light-emitting layer was spin-coated on top of the PEDOT layer using chlorobenzene as the solvent; the sample was then dried for 3 h at 60 °C *in vacuo*. Prior to film casting, the solution was filtered through a Teflon filter (0.45 μm). The TPBI layer, which was used as an electron-transporting layer that would also block holes and confine excitons, was grown through thermal sublimation in a vacuum of 3×10^{-6} Torr. The cathode was completed through thermal deposition of LiF (15 Å)/Al (100 nm). The current–voltage–luminance relationships were measured under ambient conditions using a Keithley 2400 source meter and a Newport 1835C optical meter equipped with an 818 ST silicon photodiode.

9-(*m*-Tolyl)fluoren-9-ol (1)

3-Bromotoluene (5.0 mL, 41.2 mmol) was added dropwise over 2 min to a stirred mixture of Mg (1.34 g, 54.9 mmol) and dry ether (60 mL) at ambient temperature under nitrogen. The resulting mixture was gently heated for 3 h and then 9-fluorenone (4.95 g, 27.5 mmol) in dry THF (10 mL) was added dropwise over 5 min. The solution was then heated under reflux for 12 h. After cooling, aqueous NH_4Cl solution was added and the mixture was extracted with EtOAc. The organic extracts were washed with water and brine and then dried ($MgSO_4$) The solvent was removed under reduced pressure and the residue was purified through column chromatography (hexane–EtOAc, 10 : 1) to obtain **1** (7.17 g, 96%). ^1H NMR (300 MHz, $CDCl_3$): δ 2.27 (s, 3 H), 7.01–7.03 (m, 1 H), 7.13 (dd, $J = 3.9$, 0.9 Hz, 2 H), 7.20–7.26 (m, 3 H), 7.30–7.37 (m, 4 H), 7.65 (d, $J = 7.5$ Hz, 2 H). ^{13}C NMR (75 MHz, $CDCl_3$): δ 21.4, 83.4, 119.9, 122.4, 124.6, 125.8, 127.8, 127.9, 128.2, 128.8, 137.6, 139.4, 143.0, 150.4. HRMS (*m*/*z*): calcd for $C_{20}H_{16}O$ 272.1201; found, 272.1202.

9-(3-Carboxyphenyl)fluoren-9-ol (2)

$KMnO_4$ (61.7 g, 0.31 mol) was added in four portions at intervals of 12 h to a solution of **1** (7.10 g, 26.1 mmol), pyridine (160 mL),

and water (16 mL) under reflux. After a total period of 48 h, the mixture was filtered and the solids washed with copious hot water. The filtrate was acidified with 12 N HCl and then extracted with EtOAc–Et_2O (1 : 1). The organic extracts were washed with water and brine and then dried ($MgSO_4$). The solvent was evaporated under reduced pressure and the residue was purified through column chromatography (hexane–Me_2CO, 8 : 1) to afford **2** (7.88 g, 75%). ^{1}H NMR (300 MHz, CD_3COCD_3): δ 7.26–7.41 (m, 8 H), 7.61–7.64 (m, 1 H), 7.81 (d, J = 7.5 Hz, 2 H), 7.94 (d, J = 7.5 Hz, 1 H), 8.19 (s, 1 H). ^{13}C NMR (75 MHz, CD_3COCD_3): δ 84.3,121.5,126.1,128.1,129.6,129.7, 129.73,130.3,131.5,131.8,141.1,147.0,152.5,168.4. HRMS (*m*/*z*): calcd for $C_{20}H_{14}O_3$ 302.0943; found, 302.0937.

9-(3-Carboxyphenyl)-9-(4-diphenylaminophenyl)fluorene (3)

CH_3SO_3H (40 μL, 660 μmol) was added dropwise under nitrogen to a solution of **2** (200 mg, 660 μmol) and triphenylamine (240 mg, 990 μmol) in 1,4-dioxane (3 mL) at 100 °C and then the mixture was heated at that temperature for 1 h. After this period, the reaction mixture was cooled and diluted with CH_2Cl_2. The CH_2Cl_2 solution was washed with saturated $NaHCO_{3(aq)}$ and brine and then dried ($MgSO_4$). Evaporation of the solvent followed by silica gel chromatography (hexane–Me_2CO, 3 : 1) gave **3** (250 mg, 70%). ^{1}H NMR (300 MHz, CD_3COCD_3): δ 6.92 (d, J = 8.8 Hz, 2 H), 6.98–7.04 (m, 6 H), 7.13 (d, J = 8.8 Hz, 2 H), 7.22–7.54 (m, 12 H), 7.90–7.94 (m, 4 H). ^{13}C NMR (75 MHz, CD_3COCD_3): δ 65.2, 120.8, 124.6, 124.7, 125.9, 127.7, 129.4, 129.5, 129.6, 130.1, 130.3, 130.5, 130.9, 132.2, 134.2, 140.8, 141.7, 148.2, 148.4, 149.2, 152.4, 168.2. HRMS (*m*/*z*): calcd. for $C_{38}H_{27}NO_2$ 529.2042; found, 529.2047.

9-{3-[*N*′-(4-*tert*-Butylbenzoyl)]-*N*-benzoylhydrazide}-9-(4-diphenylaminophenyl)fluorene (4)

N-Methylmorphine (0.57 mL, 5.15 mmol) and isobutylchloroformate (0.68 mL, 5.15 mmol) were added sequentially under nitrogen to a solution of **3** (2.48 g, 4.68 mmol) in THF (30 mL) at −45 °C; a white suspension formed during the addition of *i*BuOCOCl. The reaction mixture was stirred for 45 min at −45 °C before 4-*tert*-butylbenzhydrazide (0.90 g, 4.68 mmol) was added. The resulting mixture was stirred at ambient temperature for an additional 3 h before being filtered through silica gel and washed with EtOAc. The solvent was evaporated under vacuum; column chromatography of the residue (SiO_2; hexane–Me_2CO, 2 : 1) provided **4** (2.04 g, 62%). ^{1}H NMR (300 MHz, CD_3COCD_3): δ 1.35 (s, 9 H), 6.93 (d, J = 8.6 Hz, 2 H), 6.99–7.05 (m, 6 H), 7.13 (d, J = 8.6 Hz, 2 H), 7.20–7.32 (m, 7 H), 7.36–7.43 (m, 3 H), 7.49–7.54 (m, 4 H), 7.88−7.99 (m, 6 H), 9.90 (br, 2 H). ^{13}C NMR (75 MHz, CD_3COCD_3): δ 32.1, 36.1, 66.4, 121.9, 124.5, 124.54, 125.8, 126.8, 127.3, 127.7, 128.6, 128.9, 129.3, 129.4, 129.9, 130.4, 130.8, 131.3, 133.0, 134.4, 140.9, 141.5, 148.0, 148.3, 149.0, 152.3, 156.5, 167.5, 167.7. HRMS (*m*/*z*): calcd. for $C_{49}H_{41}N_3O_2$ 703.3199; found, 703.3204.

9-(3-(5-(4-*tert*-Butylphenyl)-2-oxadiazoyl)phenyl)-9-(4-diphenylaminophenyl)-fluorene (5)

CBr_4 (66.0 mg, 190 μmol) and Ph_3P (52.0 mg, 190 μmol) were added under nitrogen in a single portion to a solution of **4** (70.0 mg, 90 μmol) in CH_2Cl_2 (5 mL) at ambient temperature. The mixture was heated under reflux for 6 h; after cooling, evaporation of the solvent and column chromatography of the residue (SiO_2; hexane–Me_2CO, 3 : 1) afforded **5** (42.4 mg, 62%). ^{1}H NMR (300 MHz, CD_3COCD_3): δ 1.36 (s, 9 H), 6.91–7.0 (m, 4 H), 7.04–7.09 (m, 6 H), 7.19–7.42 (m, 10 H), 7.46 (d, J = 6.0 Hz, 2 H), 7.53 (d, J = 6.0 Hz, 2 H), 7.79 (d, J = 6.0 Hz, 2 H), 7.93–7.97 (m, 1 H), 7.99 (d, J = 6.0 Hz, 2 H), 8.06 (s, 1 H). ^{13}C NMR (75 MHz, CD_3COCD_3): δ 30.1, 35.1, 65.2, 120.8, 121.7, 123.4, 123.5, 124.5, 124.6, 125.4, 126.3, 126.5, 126.9, 128.3, 128.4, 129.3, 129.7, 131.7, 139.5, 140.5, 147.0 148.0, 148.1, 151.0 155.6, 164.4, 164.7. HRMS (*m*/*z*): calcd. for $C_{49}H_{39}N_3O$ 685.3093; found, 685.3101. Anal. Calcd: C, 85.81; H, 5.73; N, 6.13. Found: C, 85.77; H, 5.77; N, 6.12%.

Preparation of tBu-OXDTFA

CH_3SO_3H (30 μL, 520 μmol) was added dropwise under nitrogen to a mixture of **5** (170 mg, 260 μmol) and **6** (180 mg, 570 μmol) in CH_2Cl_2 (5 mL) at 50 °C and then the resultant mixture was heated at that temperature for 1 h. Upon cooling, the reaction mixture was diluted with CH_2Cl_2 (20 mL), washed with saturated $NaHCO_3$ solution and water, and then dried ($MgSO_4$). Evaporation of the solvent followed by column chromatography of the residue (SiO_2; hexane–Me_2CO, 3 : 1) gave **tBu-OXDTFA** (240 mg, 75%). ^{1}H NMR (500 MHz, CD_3COCD_3): δ 1.21 (s, 18 H), 1.34 (s, 9 H), 6.84–6.86 (m, 6 H), 7.03 (d, J = 8.5 Hz, 4 H), 7.06 (d, J = 8.5 Hz, 6 H), 7.22–7.25 (m, 8 H), 7.28–7.35 (m, 6 H), 7.38–7.41 (m, 6 H), 7.44–7.49 (m, 4 H), 7.60 (d, J = 8.5 Hz, 2 H), 7.83 (d, J = 8.0 Hz, 4 H), 7.89 (d, J = 8.0 Hz, 2 H), 7.95–7.98 (m, 4 H). ^{13}C NMR (75 MHz, CD_3COCD_3): δ 30.8, 31.1, 34.3, 35.1, 64.2, 65.1, 120.5, 120.8, 121.6, 123.3, 124.0, 124.5, 125.4, 125.5, 126.1, 126.5, 126.8, 127.8, 127.9, 128.0, 128.2, 128.3, 129.1, 129.3, 129.7, 131.8, 139.3, 140.3, 140.4, 140.7, 143.3, 146.0, 146.5, 148.0, 149.4, 150.9, 151.6, 155.5, 164.4, 164.7. HRFAB MS (*m*/*z*): calcd. for $C_{95}H_{79}N_3O$ 1277.6223; found, 1277.6239. Anal. Calcd: C, 89.24; H, 6.23; N, 3.29. Found: C, 88.78; H, 6.23; N, 3.37%.

Acknowledgements

This study was supported generously by the National Science Council, Republic of China.

References

1 T. Fuhrmann and J. Salbeck, *MRS Bull.*, 2003, **28**, 354.
2 (*a*) C. Adachi, M. A. Baldo, M. E. Thompson and S. R. Forrest, *J. Appl. Phys.*, 2001, **90**, 5048; (*b*) Y. Kawamura, K. Goushi, J. Brooks, J. J. Brown, H. Sasabe and C. Adachi, *Appl. Phys. Lett.*, 2005, **86**, 071104.
3 (*a*) M. A. Baldo, C. Adachi and S. R. Forrest, *Phys. Rev. B*, 2000, **62**, 10967; (*b*) F.-C. Chen, Y. Yang, M. E. Thompson and J. Kido, *Appl. Phys. Lett.*, 2002, **80**, 2308.
4 (*a*) M. T. Bernius, M. Inbasekaran, J. O'Brien and W. Wu, *Adv. Mater.*, 2000, **12**, 1737; (*b*) A. Adronov and J. M. J. Fréchet, *Chem. Commun.*, 2000, 1701; (*c*) L. Akcelrud, *Prog. Polym. Sci.*, 2003, **28**, 875; (*d*) J. Ding, J. Gao, Y. Cheng, Z. Xie, L. Wang, D. Ma, X. Jing and F. Wang, *Adv. Funct. Mater.*, 2006, **16**, 575; (*e*) P. L. Burn, S.-C. Lo and I. D. W. Samuel, *Adv. Mater.*, 2007, **19**, 1675.
5 (*a*) J. Kido, K. Hongawa, K. Okuyama and K. Nagai, *Appl. Phys. Lett.*, 1994, **64**, 815; (*b*) S. Lamansky, P. I. Djurovich, F. Abdel-Razzaq, S. Garon, D. L. Murphy and M. E. Thompson, *J. Appl. Phys.*, 2002, **92**, 1570; (*c*) F.-I. Wu, H.-J. Su, C.-F. Shu, L. Luo,

W.-G. Diau, C.-H. Cheng, J.-P. Duan and G.-H. Lee, *J. Mater. Chem.*, 2005, **15**, 1035.
6 (*a*) T.-H. Kim, H. K. Lee, O. O. Park, B. D. Chin, S.-H. Lee and J. K. Kim, *Adv. Funct. Mater.*, 2006, **16**, 611; (*b*) H. Kim, Y. Byun, R. R. Das, B.-K. Choi and P.-S. Ahn, *Appl. Phys. Lett.*, 2007, **91**, 093512.
7 (*a*) C. Rullière and P. C. Roberge, *Chem. Phys. Lett.*, 1983, **97**, 247; (*b*) T. F. Palmer and S. S. Parmar, *J. Photochem.*, 1985, **31**, 273; (*c*) K. Brunner, A. van Dijken, H. Börner, J. J. A. M. Bastiaansen, N. M. M. Kiggen and B. M. W. Langeveld, *J. Am. Chem. Soc.*, 2004, **126**, 6035.
8 (*a*) C.-F. Shu, R. Dodda, F.-I. Wu, M. S. Liu and A. K.-Y. Jen, *Macromolecules*, 2003, **36**, 6698; (*b*) F.-I. Wu, P.-I. Shih, C.-F. Shu, Y.-L. Tung and Y. Chi, *Macromolecules*, 2005, **38**, 9028.
9 (*a*) T. Ohta, K. Shudo and T. Okamoto, *Tetrahedron Lett.*, 1983, **24**, 71; (*b*) P.-I. Shih, C.-L. Chiang, A. K. Dixit, C.-K. Chen, M.-C. Yuan, R.-Y. Lee, C.-T. Chen, E. W.-G. Diau and C.-F. Shu, *Org. Lett.*, 2006, **8**, 2799.
10 H. A. Rajapakse, H. Zhu, M. B. Young and B. T. Mott, *Tetrahedron Lett.*, 2006, **47**, 4827.
11 E. Weber, N. Doerpinghaus and I. Csoeregh, *J. Chem. Soc., Perkin Trans. 2*, 1990, 2167.
12 J. C. Sancho-Garaía, C. L. Foden, I. Grizzi, G. Greczynski, M. P. De Jong, W. R. Salaneck, J. L. Brédas and J. Cornil, *J. Phys. Chem. B*, 2004, **108**, 5594.
13 Y.-L. Tung, P.-C. Wu, C.-S. Liu, Y. Chi, J.-K. Yu, Y.-H. Hu, P.-T. Chou, S.-M. Peng, G.-H. Lee, Y. Tao, A. J. Carty, C.-F. Shu and F.-I. Wu, *Organometallics*, 2004, **23**, 3745.
14 (*a*) Y.-Y. Chien, K.-T. Wong, P.-T. Chou and Y.-M. Cheng, *Chem. Commun.*, 2002, 2874; (*b*) K.-T. Wong, S.-Y. Ku, Y.-M. Cheng, X.-Y. Lin, Y.-Y. Hung, S.-C. Pu, P.-T. Chou, G.-H. Lee and S.-M. Peng, *J. Org. Chem.*, 2006, **71**, 456.
15 R. J. Holmes, S. R. Forrest, Y.-J. Tung, R. C. Kwong, J. J. Brown, S. Garon and M. E. Thompson, *Appl. Phys. Lett.*, 2003, **82**, 2422.
16 P.-I. Shih, C.-H. Chien, F.-I. Wu and C.-F. Shu, *Adv. Funct. Mater.*, 2007, **17**, 3514.

